ISSN 0915-633X

INTERNATIONAL ATOMIC ENERGY AGENCY

17th IAEA Fusion Energy Conference
Yokohama, Japan, 19 - 24 October 1998

IAEA-CN-69/EX2/2

NATIONAL INSTITUTE FOR FUSION SCIENCE

Transition from L Mode to High Ion Temperature Mode in CHS Heliotron/Torsatron Plasmas

K. Ida, M. Osakabe, K. Tanaka, T. Minami, S. Nishimura, S. Okamura, A. Fujisawa, Y. Yoshimura, S. Kubo, R. Akiyama, D.S.Darrow, H. Idei, H. Iguchi, M. Isobe, S. Kado, T. Kondo, S. Lee, K. Matsuoka, S. Morita, I. Nomura, S. Ohdachi, M. Sasao, A. Shimizu, K. Tumori, S. Takayama, M. Takechi, S. Takagi, C. Takahashi, K. Toi and T. Watari

(Received - Oct. 2, 1998)

NIFS-567 Oct. 1998

RESEARCH REPORT
NIFS Series

NAGOYA, JAPAN

TRANSITION FROM L MODE TO HIGH ION TEMPERATURE MODE IN CHS HELIOTRON/TORSATRON PLASMAS

K.IDA, M.OSAKABE, K.TANAKA, T.MINAMI, S.NISHIMURA, S.OKAMURA, A.FUJISAWA, Y.YOSHIMURA, S.KUBO, R.AKIYAMA, D.S.DARROW[1)], H.IDEI,. H.IGUCHI, M.ISOBE, S.KADO, T.KONDO[2)], S.LEE, K.MATSUOKA, S.MORITA, I.NOMURA, S.OHDACHI, M.SASAO, A.SHIMIZU[3)], K.TUMORI, S.TAKAYAMA[2)], M.TAKECHI[3)], S.TAKAGI[3)], C.TAKAHASHI, K.TOI, T.WATARI

National Institute for Fusion Science, Oroshi-cho, Toki-shi, Gifu, 509-5292, Japan
[1)]Princeton Plasma Physics Laboratory, Princeton, NJ 08543, U.S.A.
[2)]Graduate University for Advanced Studies, Hayama, 240-01, Japan
[3)]Dept. Energy Engineering Science, Nagoya Univ., Nagoya, 464-01, Japan

Abstract

A high ion temperature mode (high T_i mode) is observed for neutral beam heated plasmas in the Compact Helical System (CHS) Heliotron/torsatron. The high T_i mode plasma is characterized by a high central ion temperature, $T_i(0)$, and is associated with a peaked electron density profile produced by neutral beam fueling with low wall recycling. Transition from L mode to high T_i mode has been studied in CHS. The central ion temperature in the high T_i mode discharges reaches to 1 keV which is 2.5 times higher than that in the L mode discharges. The ion thermal diffusivity is significantly reduced by a factor of more than 2 - 3 in the high T_i mode plasma. The ion loss cone is observed in neutral particle flux in the energy range of 1 - 6 keV with a narrow range of pitch angle (90 ± 10 degree) in the high T_i mode. However, the degradation of ion energy confinement due to this loss cone is negligible.

1 INTRODUCTION

The high ion temperature (T_i) mode plasma is one of the improved modes in in Heliotron/torsatron and in stellarator[1,2]. It has many similar characteristics to that observed in super shots in TFTR [3], hot ion modes in JET and in JT-60 [4,5]. The high T_i mode is characterized by a high central ion temperature and low central ion thermal diffusivity, associated with a peaked electron density profile produced by neutral beam (NB) fueling with low wall recycling. Recently, similar high T_i mode discharges have been observed for neutral beam heated plasmas by turning off the gas puff at the onset of neutral beam in Heliotron-E devices[6,7]. In this paper, the characteristics of high T_i mode plasmas in CHS are described. The electron density and its profiles are measured with scanning 3 chord FIR interferometer, 24 points, YAG Thomson scattering, while the ion temperature and its profiles are measured with 30 point charge exchange spectroscopy (CXS) using fully stripped carbon[8]. The radial electric field profiles are derived from plasma potential profiles measured with Heavy Ion Beam Probe (HIBP)[9] and the poloidal rotation velocity profile and carbon pressure profile measured with CXS.

2 CHARACTERISTICS OF L MODE AND HIGH T_i MODE DISCHARGES

2-1 Ion temperature in the L mode and high T_i mode plasmas

Electron cyclotron resonance heating (ECH) pulse is used to produce a target plasma and a

neutral beam (NB) is injected for t = 40 -140ms. The helical magnetic field is 1.76T and magnetic axis is at 92.1cm, with an averaged minor radius of 17cm. The high T_i mode is obtained at low density with titanium gettering and with no gas puff during neutral beam injection (NBI). When the electron density increases in time with gas puffing, the ion temperature stays almost constant in time in the L-mode discharges. However, when there is no gas puff during the neutral beam injection, both $n_e(0)$ and $T_i(0)$ increase in time and the value of $T_i(0)$ reaches 0.7-0.8 keV at t = 70ms then gradually decays in time as the electron density increases. As in seen in Fig. 1, the absolute value of the central electron density, $n_e(0)$, in the high T_i mode is similar to that in the early phase of L mode discharges. For example, $n_e(0)$ at t = 70ms in the L mode discharge is almost identical to $n_e(0)$ at t = 82ms in the high T_i mode discharge. On the other hand, clear differences in the n_e profiles are observed between the high T_i mode and L mode discharges. In the high T_i mode discharge, the electron density profile is peaked ($n_e/\langle n_e\rangle$ = 1.5 ~ 2.0), while it is less peaked ($n_e/\langle n_e\rangle$ =1.0 ~ 1.5) in the L mode. As shown in Fig. 2, the ion temperatures in the high T_i mode discharges are higher than that in the L mode discharges in any time slices. The increase of ion temperature in the

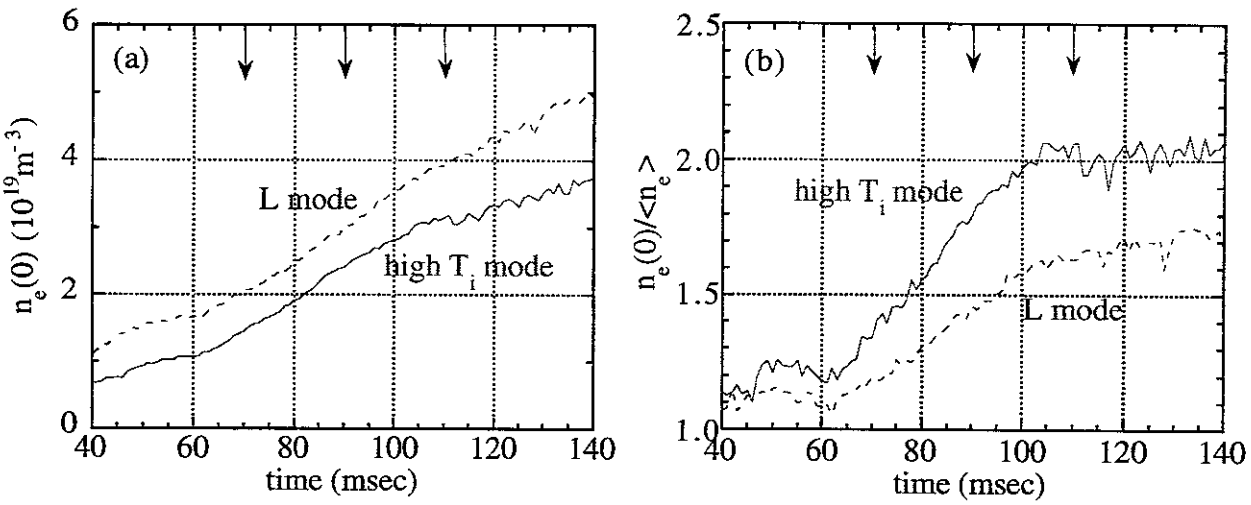

Fig.1 Time evolution of central electron density and density peaking factor $n_e/\langle n_e\rangle$, where $\langle n_e\rangle$ is the volume averaged density, for the L mode and high T_i mode discharges in CHS. Gas puff is turned off at 40 ms for the high T_i mode discharge, while there is continuous gas puffing for the L mode discharge. Arrows indicate the timing of T_i measurements with CXS.

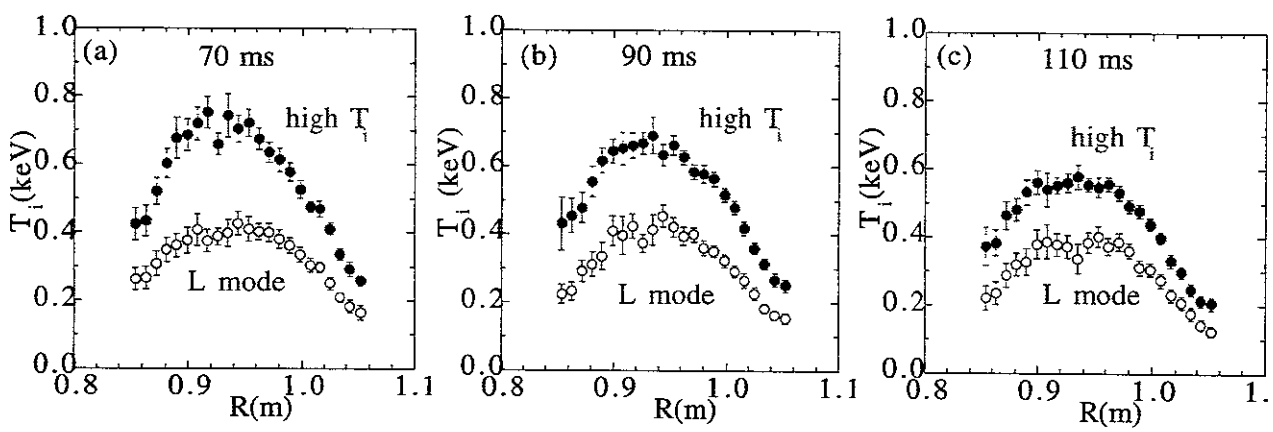

Fig.2 Radial profiles of ion temperature for L mode and high T_i mode discharges at the timing indicated by arrows in Fig.1. The plasma minor radius on the mid plane is 13cm.

high T_i mode discharges is observed in the whole plasma and in the whole duration of discharge. These data clearly show that the higher ion temperature in the high T_i mode is not due to the low electron density alone. For example, the ion temperature at 90ms in the high T_i mode discharge is significantly higher than that at t = 70ms in the L mode discharges, although the the electron density in the high T_i mode discharges is even slightly higher than in the L mode discharges at these time slices.

2-2 Ion heat transport in the high T_i mode plasma

One of the characteristic of high T_i mode is an ion temperature is as high as or even higher than the electron temperature, although the two third of the neutral beam power is deposited to the electrons. Figure 3 shows the central ion and electron temperature as a function of central electron density. Since electron density increases in time, the temperature peak appears 20 - 30 ms after the onset of NBI [t = 70ms in $T_i(0)$ and 60ms in $T_e(0)$]. It should be noted that there is almost no difference in $T_e(0)$ between L mode and high T_i mode discharges. The peaks of $T_i(0)$ are clear only in the high T_i mode discharges,and there is no peak of $T_i(0)$ in the L mode discharges, (the $T_i(0)$ is almost constant in time and does not show any density dependence). The existence of $T_i(0)$ peaks is considered to be due to the strong density dependence of $T_i(0)$ in the high T_i mode discharges. The sharp increase in the low density regime is due to the increase of deposition power (decrease of shine through and slowing down time), while the gradual decrease in the higher electron densityresults from the density dependence of transport and the sharp drop afterwards indicates the back transition from the high T_i mode to the L mode. The peak of $T_i(0)$ increases up to 1 keV as the electron density is decreased to 1.2 x 10 $^{19}m^{-3}$ (at t = 70ms) by intensive titanium gettering with a slightly higher magnetic field of 1.86T. The transport analysis has been done for the T_i profiles at t = 90ms in the high T_i mode discharge and in the L mode discharge as indicated with arrows in the Fig.3(a). The ion thermal diffusivity, χ_i , is significantly reduced in whole the plasma region and the reduction of χ_i at

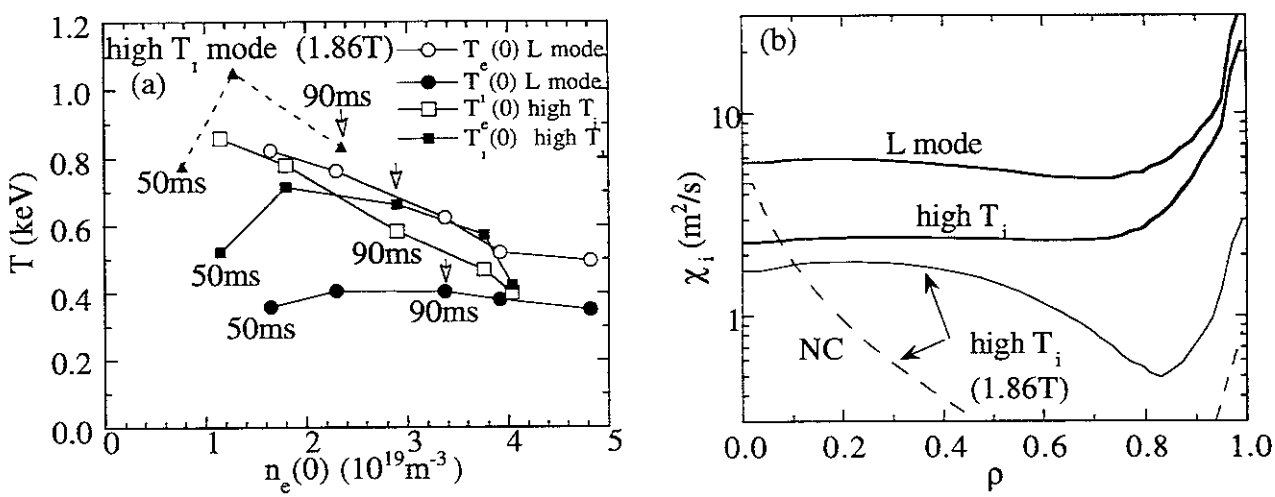

Fig.3 (a) The central ion and electron temperature in the L mode and the high T_i mode discharges with B = 1.76T and the central ion temperature in the high T_i mode discharges with B = 1.86T (also more intensive titanium gettering) as a function of central electron density and (b) radial profiles of ion thermal diffusivity in the L mode and high T_i mode discharges. Dashed line stands for the thermal diffusivity expected from neoclassical (NC) theory.

the plasma core is a factor of two to three, while there is no reduction of the electron thermal diffusivity observed in the high T_i mode plasmas. However, the measured χ_i is still higher than that expected from neoclassical theory except for the plasma center ($\rho < 0.1$) even in the high T_i mode discharges. The most region of the plasma ($\rho > 0.1$) is still dominated by the anomalous transport.

2-3. Operation regime for the high T_i mode

Fig.4(a) shows ion temperature as a function of central electron density for various levels of gas puff at t = 70, 90, 110ms. At the low density regime (t = 70 and 90 ms), there are sharp changes of $T_i(0)$ at $n_e(0) = 1.4 \times 10^{19} m^{-3}$ (t = 70ms) and $n_e(0) = 2.2 \times 10^{19} m^{-3}$ (t = 90ms), which indicates the transition from L mode to high T_i mode. The density peaking factors in the high T_i mode are 1.5 (t = 70ms) and 1.8 (t = 90ms). However, there is no sharp change (transition to the high T_i mode discharge) observed at t = 110ms because the electron density exceeds the upper limit for the high T_i mode. The high T_i mode is observed at only low density plasma and the upper limit of the electron density for the high T_i mode increases as the peaking factor of electron density is increased. The dependence of critical ne(0) on the peaking factor is more clearly seen in Fig.4(b) which shows the operation regime of high T_i mode discharges. T_i at the boundary between the high T_i mode and L mode is roughly 0.5 keV as seen in Fig4(a). The discharges with an ion temperature higher than 0.5 keV (high T_i mode plasma) are restricted to the lower $n_e(0)$ and higher ne(0)/<ne>. There is a minimum $n_e(0)$ for the high T_i mode discharges. This is mainly due to the lack of enough beam deposition and fueling at the very low density. The transition from L mode to high T_i mode is observed in the range of central electron density of $1 \times 10^{19} m^{-3}$ to $3 \times 10^{19} m^{-3}$ and the upper limit of the volume averaged electron density increases as the central electron density is increased.

2-4. Dependence of $T_i(0)$ on NBI power and magnetic field strength

The dependencies of ion temperature on NBI power and magnetic field are studied in the high T_i mode discharges. As seen in Fig.5, the central ion temperature increases as the input power of NBI is increased. The $T_i(0)$ in the high T_i mode plasmas increases gradually above the NB power of

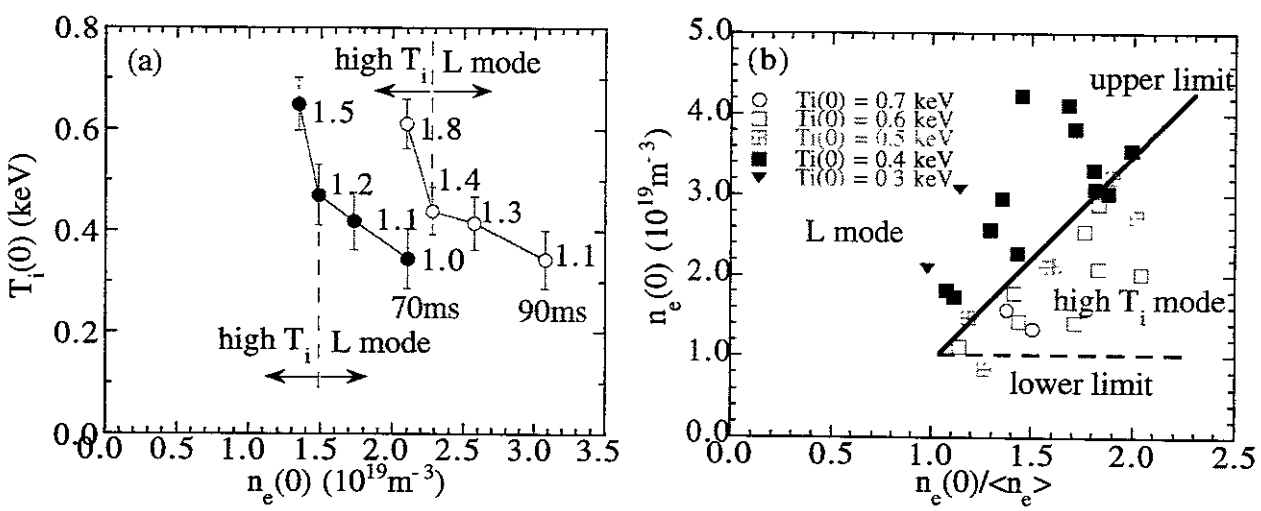

Fig.4 (a) Central ion temperature as a function of central electron density and (b) operation regime of high T_i mode discharges. The values of peaking factor $n_e(0)/<n_e>$ are also plotted in Fig.4(a).

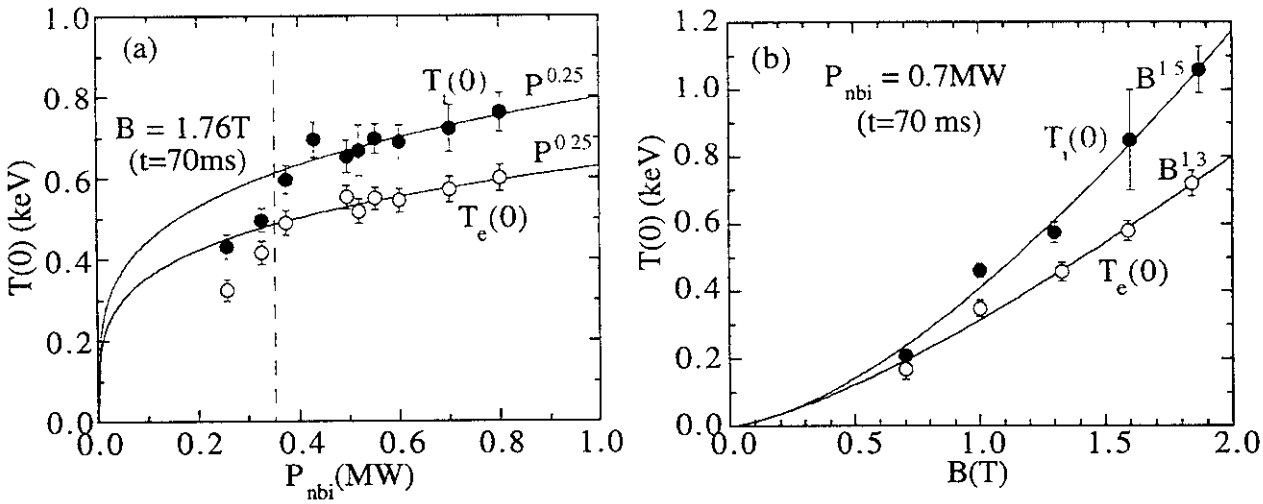

Fig.5 Central ion and electron temperatures as a function of (a) NBI heating power and (b) magnetic field strength in the high T_i mode plasmas The solid lines stand for the fitting curve for the data above 0.35MW.

0.35MW as $P^{0.25}$. However, $T_i(0)$ shows a sharp drop when the NBI power decreases below 0.35MW. This is because the density profile becomes less peaked due to the additional gas puff to keep the electron density constant in this power scan as the NBI power decreases. The central ion temperature increases up to 1.0 - 1.1 keV as the magnetic field is increased up to the maximum (1.86T). It is noted that the central ion temperature is sensitive to wall conditions and the difference in $T_i(0)$ for between 1.76T and 1.86T is not due to the change of magnetic field but due to the wall conditions. Therefore the B dependence was measured with same wall conditions in a day. The strong B dependence of $T_i(0)$ in the high T_i mode is observed. The $T_i(0)$ increases as $B^{1.5}$, while $T_e(0)$ increase as $B^{1.3}$. This strong B dependence can be explained by the fact that better particle confinement in higher magnetic field contributes to peaked density and results in more improvement of ion heat transport in addition to the linear B dependence of χ_i which is observed in L mode.

3. LOSS CONE AND RADIAL ELECTRIC FIELD IN THE T_i MODE PLASMAS

3-1 Neutral particle flux energy spectra

Because of helical ripple, there is a loss cone for fast ions with energies of a few to ten times of that of the bulk ions. The loss cone is predicted to extend to the plasma core for negative radial electric field (negative potential), while it is expected to be localized near the plasma edge for positive potential[2]. Both in the L mode and high T_i mode discharges, the loss cone exists and appears as a dip in the neutral particle energy spectra measured with neutral particle analyzer (NPA) observed perpendicular to the magnetic field (viewing angle of 12 degree) , as seen in Fig.6. The dip is more significant in the high T_i mode discharge, where the ion temperature is high. The dip becomes smaller and finally disappears when the viewing angle is tilted by up to 16 degree from the perpendicular direction. Therefore only the ions with the pitch angle of 90 ± 10 degree and with the energy of 1.5 keV [=$2T_i(0)$] escapes from the plasma due to the loss cone. The dip in the perpendicular energy spectra disappears when the radial electric field becomes positive with additional ECH [Fig. 6(b) and

Fig. 6(c)]. It is noted that the ion temperature measured with CXS, indicated as a slope in Fig. 6(a) and Fig. 6(b) , does not increase when the loss cone disappears. During ECH, the ion heating efficiency of NBI is expected to improve since a higher fraction of energy deposition to ions results from the higher electron temperature and the disappearance of loss cone in the energy range of 1 - 6 keV. However, no increase of ion temperature with ECH is observed as shown in Fig.6(c). This is because NB is injected parallel to the magnetic field (tangential injection) and the bulk plasma is heated by the slowing down of transit fast ions whose pitch angle are small enough, and loss cone in the narrow range of pitch angle (90 ±20 degree) does not affect the slowing dawn process of injected beam. The loss cone will be important for bulk ions even in the narrow range of pitch angle. This loss cone causes ion particle loss within the energy range of 1 - 6 keV. However, no change of ion temperature with and without loss cone suggests that the energy loss due to this loss cone loss is smaller than the energy loss due to ion anomalous heat transport. The loss cone loss exists in the plasma but it does not cause a degradation of ion confinement at least for the parameter range in CHS. These experiments suggest the improvement of heat transport of bulk ions is more important than the control of loss cone in optimization of the E_r profile.

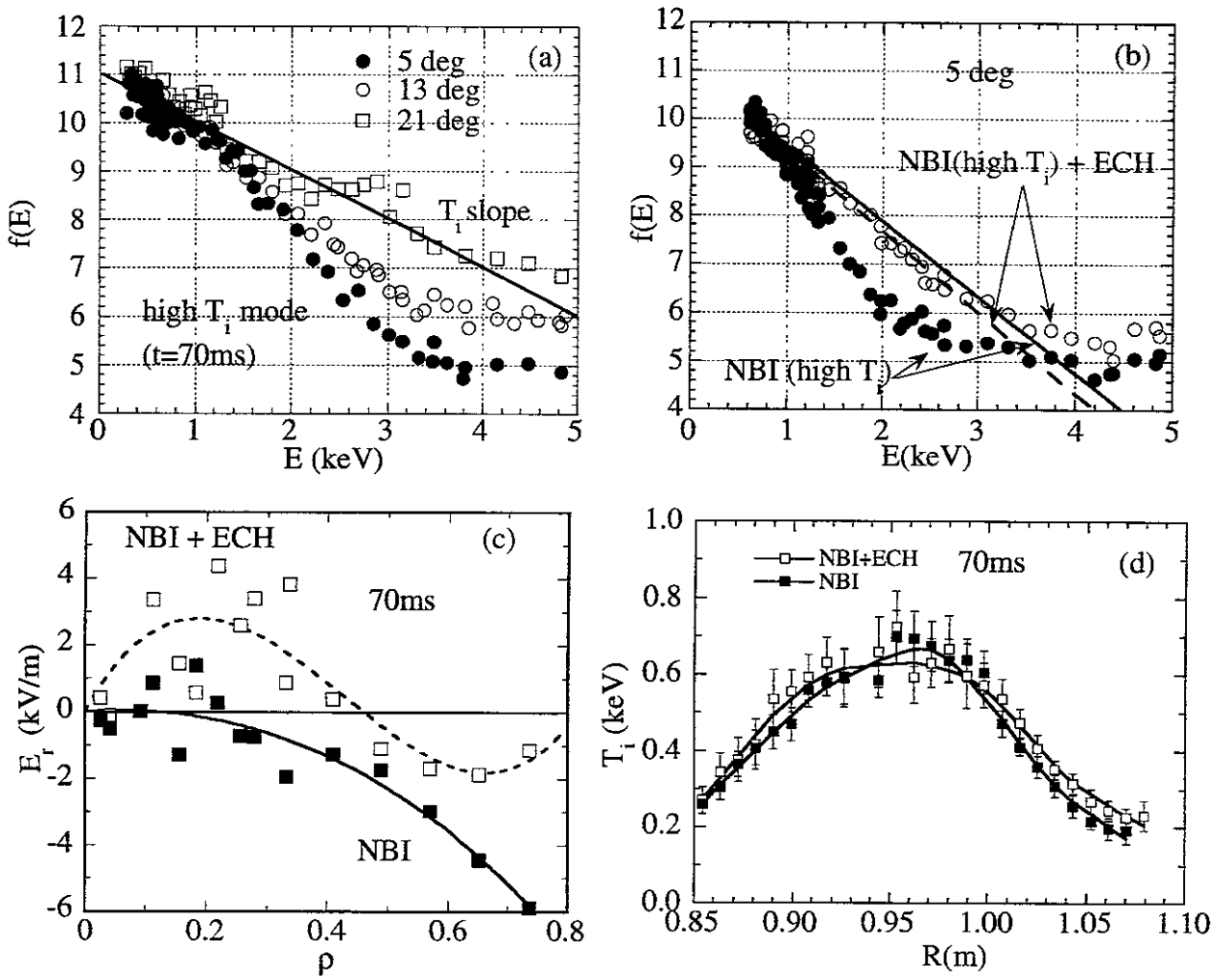

Fig.6 Neutral particle energy spectra for (a) the high T_i mode plasma with viewing angles of 12 20 and 28 degree and for (b) NBI (high T_i mode) and NBI + ECH heated plasmas. The solid and dashed lines are the slopes of energy spectra for the ion temperature measured with CXS in the NBI and NBI + ECH plasmas, respectively. Radial profiles of (c) radial electric field and (d) ion temperature for NBI (high T_i mode) and NBI + ECH heated plasmas.

3-2. Radial electric field in the L mode and high T_i mode plasmas

The radial electric field profiles can be derived from plasma potential profiles measured with HIBP and the poloidal rotation velocity profile and carbon pressure profile measured with CXS. The radial electric field measured with HIBP and CXS agree with each other as seen in Fig. 7(a). However, the agreement has not been checked in the wide range of plasma parameter. This is because the measurements of radial electric field with HIBP are restricted only to low density and a low magnetic field of 0.88T due to the limitation of beam energy and current, while the measurements of CXS require a relatively high density plasma to obtain enough charge exchange emissions. Therefore the central electron density and magnetic field in which both HIBP and CXS measurements are available, is 1 - 2 x $10^{19}m^{-3}$ and 0.88T, respectively.

The radial electric field depends on electron density and magnetic field. The radial electric field becomes more negative as the electron density is increased and magnetic field is increased. The radial electric field profiles are measured for L mode and high T_i mode discharges to study the effect of E_r on ion transport. The radial electric field becomes more negative in the high T_i mode than that in the L mode as shown in Fig. 7(a). Although the improvement of ion transport in high T_i mode with low magnetic field (0.88T) is not as good as that with high field(1.76T), the high Ti mode discharges with low magnetic field are also studied to make the HIBP measurements available. Figure 7(b) shows central ion temperature as a function of central electron density for L mode and high T_i mode discharges. In the high T_i mode discharge, the jump of ion temperature after the gas puff is turned off at t = 70ms shows the transition from L mode to high T_i mode. Figure 7(c) shows the radial electric field profiles measured with HIBP before (t=65ms) and after (t=90ms) the L to high T_i mode transition in the low magnetic field. After the transition the radial electric field becomes more negative than that in the L mode phase.

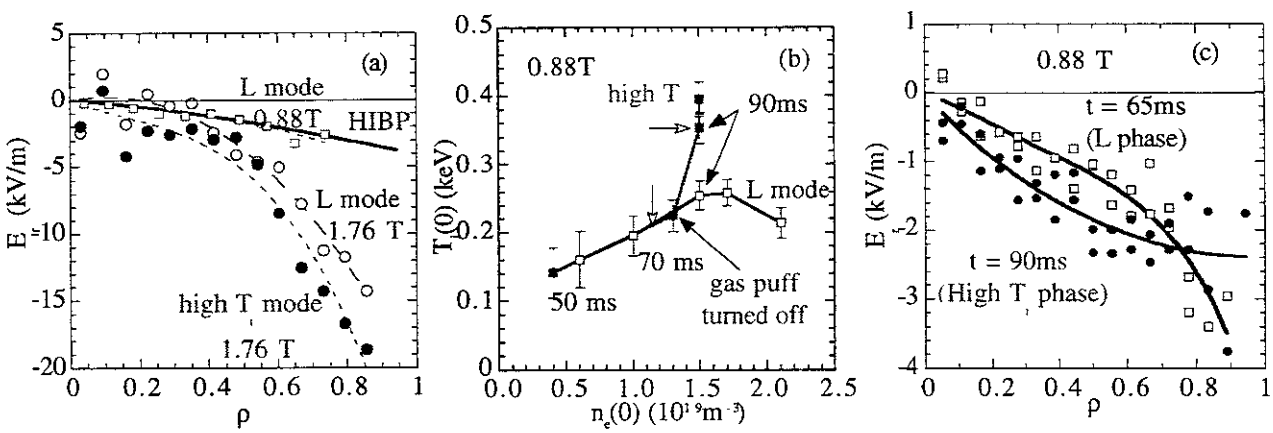

Fig.7 (a) Radial electric field for the L mode and high T_i mode with the magnetic field of 0.88T and1.76T. The solid lines stand for the radial electric field measured with HIBP, while the dashed lines stand for that measured with CXS (b) the central ion temperature as a function of central electron density for L mode and high Ti mode discharges with 0.88T, and (c) radial electric field before and after [t=65ms and 90ms as indicated with arrows in Fig7(b)] the transition from L mode to high T_i mode with the magnetic field of 0.88T.

4. Discussion

The high T_i mode discharges are characterized with peaked density profile, high ion temperature (1keV), the reduction in χ_i by a factor of more than 2 - 3 (but no reduction in χ_e), and more negative electric field. High T_i mode is observed in the low density [$n_e(0) = 1 - 3 \times 10^{19} m^{-3}$] and low recycling condition with a wide range of magnetic field and heating power. It is an important issue to investigate what causes the improvement of ion transport (not electron transport) in the high T_i mode discharges. The radial electric field shear is a candidate for explanation of the confinement improvement in the high T_i mode[10]. However, it is open to question whether the radial electric field and its shear in the high T_i mode is enough to suppress fluctuations and reduce anomalous transport. More study on radial electric field and fluctuations should be done to study the mechanism of improvement of ion transport in the high T_i mode plasmas.

The ion loss cone is observed in the energy range of 1 - 6 keV with the narrow range of pitch angle (90 ± 20 degree) in the high T_i mode. When ECH is applied to the high Ti mode plasma, the loss cone disappears but there is no increase of ion temperature observed. This observations suggests the ion loss due to loss cone, which is considered to be a disadvantage in the Heliotron/torsatron devices, does not affect ion energy confinement as long as the NB is injected tangentially. This is because the energy loss due to anomalous transport is more dominant than the ion ripple loss due to loss cone in the energy range of few times of ion temperature This seems consistent with the fact that the observed χ_i is still much higher than that expected from neoclassical theory. When the anomalous transport is suppressed to the level of neoclassical transport, the reduction of loss cone by positive radial electric field will be important. In CHS, where the anomalous transport is dominant, negative electric field would be favorable in the improvement of ion heat transport.

REFERENCES

[1] A.Iiyoshi, in Fusion Energy (Porc. 16th Int. Conf. on Fusion Energy, Montreal, 1996) IAEA Vienna Vol.1, 113 (1997).

[2] M.Kick et al., Fusion Energy (16th Conf. on Fusion Energy, Montreal, 1996) Vol.2, IAEA Vienna (1997) p27

[3] R.J.Fonck, et al., Phys. Rev. Lett. **63**, 520 (1989).

[4] H.Weisen et al., Nucl. Fusion **29**, 2187 (1989).

[5] Y.Koide, et al., Nucl. Fusion **33**, 251 (1993).

[6] K.Ida, et al., Phys. Rev. Lett. **76**, 1268 (1996).

[7] K.Ida, et al., Plasma Phys. 38, 1433 (1996).

[8] K.Ida, S.Hidekuma, Rev. Sci. Instrum. **60**, 867 (1989).

[9] A.Fujisawa, et al., in Fusion Energy (Proc. 16th Int. Conf. on Fusion Energy, Montreal, 1996) Vol.II, IAEA, Vienna, (1997) p.41.

[10] K.Ida, et al., in Fusion Energy (Proc. 16th Int. Conf. on Fusion Energy, Montreal, 1996) IAEA Vienna Vol.2 (1997).

Recent Issues of NIFS Series

NIFS-533 S Kawata, C Boonmee, T Teramoto, L. Drska, J Limpouch, R Liska, M Sinor,
Computer-Assisted Particle-in-Cell Code Development, Dec 1997

NIFS-534 Y Matsukawa, T Suda, S. Ohnuki and C. Namba,
Microstructure and Mechanical Property of Neutron Irradiated TiNi Shape Memory Alloy, Jan. 1998

NIFS-535 A. Fujisawa, H. Iguchi, H. Idei, S Kubo, K Matsuoka, S. Okamura, K. Tanaka, T. Minami, S Ohdachi, S. Monta, H. Zushi, S. Lee, M Osakabe, R. Akiyama, Y Yoshimura, K Toi, H Sanuki, K. Itoh, A. Shimizu, S. Takagi, A. Ejiri, C Takahashi, M. Kojima, S Hidekuma, K Ida, S Nishimura, N. Inoue, R Sakamoto, S -I. Itoh, Y. Hamada, M Fujiwara,
Discovery of Electric Pulsation in a Toroidal Helical Plasma; Jan 1998

NIFS-536 Lj R. Hadzievski, M.M. Skoric, M Kono and T Sato,
Simulation of Weak and Strong Langmuir Collapse Regimes, Jan. 1998

NIFS-537 H. Sugama, W. Horton,
Nonlinear Electromagnetic Gyrokinetic Equation for Plasmas with Large Mean Flows, Feb. 1998

NIFS-538 H Iguchi, T.P. Crowley, A. Fujisawa, S Lee, K. Tanaka, T Minami, S. Nishimura, K. Ida, R Akiyama, Y Hamada, H., Idei M. Isobe, M Kojima, S. Kubo, S. Monta, S Ohdachi, S Okamura, M Osakabe, K Matsuoka, C Takahashi and K Toi,
Space Potential Fluctuations during MHD Activities in the Compact Helical System (CHS); Feb 1998

NIFS-539 Takashi Yabe and Yan Zhang,
Effect of Ambient Gas on Three-Dimensional Breakup in Coronet Formation Process, Feb. 1998

NIFS-540 H. Nakamura, K. Ikeda and S. Yamaguchi,
Transport Coefficients of InSb in a Strong Magnetic Field, Feb. 1998

NIFS-541 J. Uramoto,
Development of ν_μ Beam Detector and Large Area ν_μ Beam Source by H_2 Gas Discharge (I); Mar. 1998

NIFS-542 J Uramoto,
Development of $bar\{\nu\}_\mu$ Beam Detector and Large Area $bar\{\nu\}_\mu$ Beam Source by H_2 Gas Discharge (II); Mar. 1998

NIFS-543 J. Uramoto,
Some Problems inside a Mass Analyzer for Pions Extracted from a H_2 Gas Discharge, Mar 1998

NIFS-544 J Uramoto,
Simplified ν_μ $bar\{\nu\}_\mu$ Beam Detector and ν_μ $bar\{\nu\}_\mu$ Beam Source by Interaction between an Electron Bunch and a Positive Ion Bunch; Mar. 1998

NIFS-545 J. Uramoto,
Various Neutrino Beams Generated by D_2 Gas Discharge; Mar.1998

NIFS-546 R Kanno, N. Nakajima, T. Hayashi and M. Okamoto,
Computational Study of Three Dimensional Equilibria with the Bootstrap Current; Mar 1998

NIFS-547 R Kanno, N. Nakajima and M. Okamoto,
Electron Heat Transport in a Self-Similar Structure of Magnetic Islands; Apr 1998

NIFS-548 J.E. Rice,
Simulated Impurity Transport in LHD from MIST; May 1998

NIFS-549 M.M Skoric, T. Sato, A.M Maluckov and M.S Jovanovic,
On Kinetic Complexity in a Three-Wave Interaction; June 1998

NIFS-550 S Goto and S Kida,
Passive Saclar Spectrum in Isotropic Turbulence: Prediction by the Lagrangian Direct-interaction Approximation; June 1998

NIFS-551 T. Kuroda, H. Sugama, R Kanno, M. Okamoto and W Horton,
Initial Value Problem of the Toroidal Ion Temperature Gradient Mode ; June 1998

NIFS-552 T. Mutoh, R. Kumazawa, T. Seki, F. Simpo, G. Nomura, T Ido and T. Watari,
Steady State Tests of High Voltage Ceramic Feedthoughs and Co-Axial Transmission Line of ICRF Heating System for the Large Helical Device ; June 1998

NIFS-553 N. Noda, K. Tsuzuki, A. Sagara, N. Inoue, T. Muroga,
oronaization in Future Devices -Protecting Layer against Tritium and Energetic Neutrals-: July 1998

NIFS-554 S. Murakami and H. Saleem,
Electromagnetic Effects on Rippling Instability and Tokamak Edge Fluctuations; July 1998

NIFS-555 H. Nakamura , K. Ikeda and S. Yamaguchi,
Physical Model of Nernst Element; Aug. 1998

NIFS-556 H. Okumura, S. Yamaguchi, H. Nakamura, K. Ikeda and K. Sawada,
Numerical Computation of Thermoelectric and Thermomagnetic Effects; Aug 1998

NIFS-557 T. Yasuhiko, O. Masaki, T. Katsuyoshi, O. Yoshihide, K. Osamu, A. Eiji, K. Toshikazu, A. Ryuichi and T. Masanobu,
Development of a High-Current Hydrogen-Negative Ion Source for LHD-NBI System; Aug.1998

NIFS-558 M. Tanaka, A. Yu Grosberg and T. Tanaka,
Molecular Dynamics of Structure Organization of Polyampholytes;Sep. 1998

NIFS-559 R. Horiuchi, K. Nishimura and T. Watanabe,
Kinetic Stabilization of Tilt Disruption in Field-Reversed Configurations; Sep 1998
(IAEA-CN-69/THP1/11)

NIFS-560 S. Sudo, K. Kholopenkov, K. Matsuoka, S. Okamura, C. Takahashi, R. Akiyama, A. Fujisawa, K. Ida, H Idei, H. Iguchi, M. Isobe, S. Kado, K. Kondo, S. Kubo, H. Kuramoto, T. Minami, S. Morita, S. Nishimura, M. Osakabe, M. Sasao, B Peterson, K. Tanaka, K. Toi and Y. Yoshimura,
Particle Transport Study with Tracer-Encapsulated Solid Pellet Injection;Oct. 1998
(IAEA-CN-69/EXP1/18)

NIFS-561 A. Fujisawa, H. Iguchi, S. Lee, K. Tanaka, T. Minami, Y. Yoshimura, M. Osakabe, K. Matsuoka, S. Okamura, H. Idei, S. Kubo, S. Ohdachi, S. Morita, R. Akiyama, K. Toi, H. Sanuki, K. Itoh, K. Ida, A. Shimizu, S. Takagi, C. Takahashi, M. Kojima, S. Hidekuma, S. Nishimura, M. Isobe, A. Ejiri, N. Inoue, R. Sakamoto, Y. Hamada and M. Fujiwara,
Dynamic Behavior Associated with Electric Field Transitions in CHS Heliotron/Torsatron; Oct. 1998
(IAEA-CN-69/EX5/1)

NIFS-562 S. Yoshikawa,
Next Generation Toroidal Devices; Oct 1998

NIFS-563 Y. Todo and T. Sato,
Kinetic-Magnetohydrodynamic Simulation Study of Fast Ions and Toroidal Alfvén Eigenmodes; Oct. 1998
(IAEA-CN-69/THP2/22)

NIFS-564 T. Watari, T. Shimozuma, Y. Takeiri, R Kumazawa, T. Mutoh, M. Sato, O. Kaneko, K. Ohkubo, S. Kubo, H. Idei, Y. Oka, M. Osakabe, T. Seki, K. Tsumori, Y Yoshimura, R. Akiyama, T. Kawamoto, S. Kobayashi, F Shimpo, Y. Takita, E Asano, S. Itoh, G Nomura, T. Ido, M. Hamabe, M. Fujiwara, A. Iiyoshi, S. Morimoto, T Bigelow and Y P. Zhao,
Steady State Heating Technology Development for LHD; Oct. 1998
(IAEA-CN-69/FTP/21)

NIFS-565 A. Sagara, K.Y. Watanabe, K. Yamazaki, O. Motojima, M. Fujiwara, O. Mitarai, S. Imagawa, H. Yamanishi, H. Chikaraishi, A. Kohyama, H. Matsui, T. Muroga, T. Noda, N. Ohyabu, T Satow, A.A. Shishkin, S. Tanaka, T. Terai and T Uda,
LHD-Type Compact Helical Reactors;Oct. 1998
(IAEA-CN-69/FTP/03(R)

NIFS-566 N. Nakajima, J Chen, K Ichiguchi and M. Okamoto,
Global Mode Analysis of Ideal MHD Modes in L=2 Heliotron/Torsatron Systems;Oct. 1998
(IAEA-CN-69/THP1/08)

NIFS-567 K. Ida, M. Osakabe, K. Tanaka, T. Minami, S. Nishimura, S. Okamura, A. Fujisawa, Y. Yoshimura, S. Kubo, R. Akiyama, D.S.Darrow, H. Idei, H. Iguchi, M. Isobe, S. Kado, T. Kondo, S. Lee, K. Matsuoka, S. Morita, I. Nomura, S. Ohdachi, M. Sasao, A. Shimizu, K. Tumori, S. Takayama, M. Takechi, S. Takagi, C. Takahashi, K. Toi and T. Watari,
Transition from L Mode to High Ion Temperature Mode in CHS Heliotron/Torsatron Plasmas;Oct. 1998
(IAEA-CN-69/EX2/2)